Hindawi Publishing Corporation
Journal of Nanomaterials
Volume 2016, Article ID 9159364, 8 pages
http://dx.doi.org/10.1155/2016/9159364

Research Article

Preparation and Characterization of Vancomycin-Loaded Electrospun *Rana chensinensis* Skin Collagen/Poly(L-lactide) Nanofibers for Drug Delivery

Mei Zhang,[1] Ziqi Li,[1,2] Lihua Liu,[2] Zhouyang Sun,[2] Wendi Ma,[2] Zhichao Zhang,[2] Rui Zhang,[2] and Dahui Sun[3]

[1]*Alan G. MacDiarmid Laboratory, College of Chemistry, Jilin University, Changchun 130012, China*
[2]*College of Quartermaster Technology, Jilin University, Changchun 130062, China*
[3]*Norman Bethune First Hospital, Jilin University, Changchun 130021, China*

Correspondence should be addressed to Dahui Sun; sundahui1971@sina.com

Received 24 May 2016; Accepted 19 July 2016

Academic Editor: Zeeshan Khatri

Collagen was extracted from abandoned *Rana chensinensis* skin in northeastern China via an acid enzymatic extraction method for the use of drug carriers. In this paper we demonstrated two different nanofiber-vancomycin (VCM) systems, that is, VCM blended nanofibers and core-shell nanofibers with VCM in the core. *Rana chensinensis* skin collagen (RCSC) and poly(L-lactide) (PLLA) (3 : 7) were blended in 1,1,1,3,3,3-hexafluoroisopropanol (HFIP) at a concentration of 10% (g/mL) to fabricate coaxial and blend nanofibers, respectively. Coaxial and blend electrospun RCSC/PLLA nanofibers containing VCM (5 wt%) were evaluated for the local and temporal delivery of VCM. The nanofiber scaffolds were characterized by environmental scanning electron microscope (ESEM), transmission electron microscopy (TEM), Fourier transform infrared spectra (FTIR), differential scanning calorimeter (DSC), water contact angle (WCA), and mechanical tests. The drug release of VCM in these two systems was compared by using UV spectrophotometer. The empirical result indicated that both the blend and coaxial RCSC/PLLA scaffolds followed sustained control release for a period of 80 hours, but the coaxial nanofiber might be a potential drug delivery material for its better mechanical properties and sustained release effect.

1. Introduction

Preventing wound infection has been the major difficulty in wound care field in recent years [1]. Open skin wound is a potential invasion site which may result in the invasion of the bacteria and pathogens [2]. Infectious organisms preferentially target wounds beneath dressing materials, leading to possibly serious infections that require removal of the wound dressing and excision of cutaneous wounds [3]. Thus, effective and nontoxic antibacterial materials composed of biological components have attracted much attention in recent years [4]. Cast films [5], nanoparticles [6], and nanofibers [7] have been investigated for drug carriers. Among various of antibacterial materials, electrospun nanofibers with the characteristics of fiber controllable size, large specific surface area, high porosity, and unique characteristics of three-dimensional network structure could excellently simulate the natural extracellular matrix (EMC) and have been widely used in tissue engineering scaffolds, tissue repair, drug carrier, and so on [8]. In addition, it has been proved that electrospun nanofiber is an efficient drug delivery system [9].

Collagen is abundant in connected tissue such as skin, bones, tendons, ligaments, and blood vessels in animals [10, 11]. Cattle and pigs have always been the main source of collagen. However, the threat of animal diseases such as mad cow disease and foot-and-mouth disease became a problem and people with special religion or custom cannot use terrestrial source collagen, so to look for new alternative sources is urgent and it is becoming a hot spot of research to extract collagen from marine organism [12].

Rana chensinensis, a kind of primitive animal in northeastern China, is widely used in edible and medical fields for its high nutritive value [13]. However, large quantities of waste skin of *R. chensinensis* become a problem [14, 15]. The skin of *R. chensinensis* contains numerous bioactive substances with great application value and exploitation potential. People have already purified helpful substance such as polysaccharide and antimicrobial peptides from the abandoned *Rana chensinensis* skin [14–16]. In our previous work, *Rana chensinensis* skin collagen (RCSC) was isolated and purified by acid enzyme extraction [17]. Poly(L-lactide) (PLLA), a kind of synthetic materials, which improves mechanical properties along with good biodegradability and bioabsorbability, can cause complementary performance and synergy with the collagen [18]. In this paper, the RCSC and PLLA are used for the fabrication of nanofiber scaffolds.

Vancomycin (VCM) is a glycopeptide antibiotic that functions by inhibiting the formation of the bacterial cell wall [19]. It is effective against gram-positive bacteria, especially in recalcitrant staphylococcal infections that are unresponsive to penicillin or cephalosporin antibiotics [20].

Nanofibers with different structure may exhibit different drug release effect. Two different electrospun processes of this paper were introduced to study the drug release in nanofibers, that is, blend electrospun [9] and coaxial electrospun [21]. In this study, VCM, as a model drug, was encapsulated into RCSC/PLLA nanofibers by two different electrospinning processes to impart controlled release of VCM. Characteristic and properties as well as drug release of the two different types of nanofibers were studied in this research.

2. Experimental

2.1. Materials. Skin samples were collected from the residues of *Rana chensinensis* in the northeastern China. Collagen was extracted from the skin samples through acid enzymatic extraction in our lab [17]. PLLA with an average molecular weight (Mw) of 180,000 was purchased from Jinan Dai Gang Biotechnology Co., Ltd., China, and vancomycin was provided by Hefei Bo Biotechnology Co., Ltd., China. 1,1,1,3,3,3-Hexafluoro-2-propanol (HFIP) from Energy Chemical Co., China, was used to dissolve the RCSC, PLLA, VCM, and their blends.

2.2. Preparation and Electrospinning. Coaxial electrospinning was employed to produce core-shell nanofiber system with VCM in the core and uniaxial electrospinning was introduced for the blend nanofibers. For the coaxial nanofiber-VCM system, the core solution was prepared by dissolving 0.065 g of PLLA and 0.005 g of VCM in 0.5 mL of HFIP. And the shell solution was prepared by dissolving 0.03 g of RCSC in 0.5 mL of HFIP. For the blend nanofiber-VCM system, the complex composed of PLLA (0.064 g), RCSC (0.03 g), and VCM (0.005 g) was dissolved in HFIP (1 mL) solutions.

All solutions were stirred in the magnetic stirrer for 6 h before electrospinning. For the coaxial nanofibers, the RCSC solutions and PLLA (VCM) solutions were transferred into 1 mL plastic syringe with an 18-gauge outer needle of and a 25-gauge inner needle of, respectively. The flow rates of the RCSC and PLLA (VCM) were 1.2 mL/h and 0.9 mL/h. For the blend uniaxial nanofibers, the blend RCSC/PLLA/VCM solutions were transferred into 1 mL plastic syringe with a 25-gauge needle at a flow rate of 2.1 mL/h. A clamp connected the high voltage power supplier of 15 kV to the needle. A piece of aluminum foil was placed at 125 mm directly below the needle to act as a collector.

2.3. Characterization of Nanofibers

2.3.1. Environmental Scanning Electron Microscope (ESEM). The morphology of the electrospun nanofiber scaffolds was observed by using an environment scanning electron microscopy (ESEM) XL-30 ESEM (FEI, Co., Ltd., American) at an accelerating voltage of 15 kV after gold coating. Based on the SEM micrographs, the nanofiber diameter was determined by choosing 100 fibers at random from 5000x magnification SEM images and image was analyzed by Nano Measurer 1.2 (Fudan University, China).

2.3.2. Transmission Electron Microscopy (TEM). The core-shell structure of the coaxial RCSC/PLLA nanofiber was verified by transmission electron microscopy (TEM) S-3400N TEM (HI TACHI, Japan) at accelerating of 110 kv. The nanofiber was collected by the 400-mesh copper network.

2.3.3. Fourier Transform Infrared Spectra (FTIR). Fourier transform infrared spectra (FTIR) studies were carried out on compressed films containing KBr (200 mg) and samples (10 mg) using a FTIR spectrophotometer (IRTracer-100, SHIMADZU). Spectra in the 400 to 4000 cm^{-1} range were measured.

2.3.4. Differential Scanning Calorimeter (DSC). The thermal behavior of electrospun PLLA and RCSC/PLLA nanofiber membranes was tested by differential scanning calorimetry (DSC) (821e, Mettler-Toledo, Germany) in the protection of nitrogen gas with the flow rate of 100 mL/min at room temperature. The sample was about 2.5 mg. The samples were scanned at a heating rate of 10°C/min within 25–200°C. The degree of crystallinity was obtained by using the following equation:

$$X_c\% = \frac{1}{\left(1 - m_f\right)} \left[\frac{\Delta H_m - \Delta H_c}{\Delta H_0}\right] \times 100\%, \quad (1)$$

where ΔH_m is the melting enthalpy, ΔH_c is the cold crystallization enthalpy, ΔH_0 is the melting enthalpy of totally crystallized PLLA, taken as 93 J/g, and $(1 - m_f)$ is the weight fraction of PLLA in the sample.

2.3.5. Water Contact Angle (WCA). The contact angle of the scaffolds was investigated by using an angle contact measurement XG-GAM at room temperature at 0 s, 5 s, and 10 s by pendant drop method. The contact angle between the scaffolds and the pure water was measured. Before the test, the scaffolds were cut into a square of 20 mm × 40 mm.

2.3.6. Mechanical Measurements. A tabletop LLY-06ED tester with a maximum strength length of 10 mm was used to determine the tensile properties of electrospun matrix at ambient temperature with a speed of 5 mm/min. Before the mechanical tests, the electrospun RCSC/PLLA nanofibers tubes were first cut along the length direction into rectangular specimens with a typical size of 50 mm (lengthwise) × 5 mm (widthwise). The thickness of each specimen was measured by micrometers with a precision of 0.001 mm.

2.4. Release Behaviors. A testing machine UV-vis spectrophotometer (UV-2600 Co., Ltd., Japan) was employed to measure the release behavior of VCM in the nanofiber membrane. The nanofiber membranes with weight of 15 mg were placed into 30 mL phosphate buffer solution and incubated at 60 rpm at 37°C in a thermostatically shaking incubator. Aliquots of 1 mL were retrieved in predetermined time intervals and an equal volume of fresh PBS was added to the suspension. The VCM concentration of each sample was calculated using a standard curve, relating the quantity of VCM with the intensity of light absorbance. Samples of 1 mL were taken at predefined time at 20 min, 40 min, 60 min, 100 min, 150 min, 210 min, 5 h, 7 h, 10 h, 22 h, 29 h, 36 h, 48 h, 54 h, 75 h, and 100 h, respectively. All experiments were done in triplicate.

3. Results and Discussion

3.1. Morphology of Nanofibers. Figure 1 shows the SEM micrographs and fiber diameter distributions of these four electrospun scaffolds. All nanofibers showed continuous and bead-free morphology. It is obvious that the nanofiber scaffolds exhibited uniform diameter distribution with ultrafine nanofibers except the coaxial RCSC/PLLA nanofibers. The average diameters of the blend and coaxial RCSC/PLLA nanofibers are 583.4 ± 162.4 nm and 698.2 ± 195.0 nm while the blend and coaxial RCSC/PLLA/VCM nanofibers are 551.8 ± 248.6 nm and 669.7 ± 192.6 nm. Coaxial nanofiber has higher average diameters than the blend group which may contribute to the different way of electrospinning. With the addition of VCM, both the blend and coaxial nanofiber diameter decreased and irregular fibers were clearly observed in Figures 1(b1) and 1(d1). Some authors also found the phenomenon that while the VCM was adding to the polymer, the diameter of the polymer decreased [22]. One explanation of this phenomenon may be that the addition of VCM decreases the continuity of the blend and probably affected the mechanical properties of the nanofiber matrix. However, we can also observe that, with the addition of VCM in Figures 1(b1) and 1(d1), the amount of surface roughness decreased. This showed that the RCSC, PLLA, and VCM were dissolved in HFIP uniformly without agglomeration.

TEM micrographs of the coaxial nanofibers were shown in Figure 2. Both the coaxial RCSC/PLLA and VCM-loaded coaxial RCSC/PLLA nanofibers showed obvious core-shell structure and the nanofiber diameter decreased with the addition of VCM in the core.

3.2. FTIR Spectroscopy. The FTIR spectrum is an effective method to define the existence of the scaffolds component. The FTIR spectra of the electrospun PLLA, RCSC, VCM, and their blends nanofibers are shown in Figure 3. From Figure 3(a), three characteristic peaks of RCSC at 1658 cm^{-1}, 1537 cm^{-1}, and 1261 cm^{-1} corresponded to amide I, amide II, and amide III of the collagen, respectively [23]. Among them, amide I band is caused by C–O stretching vibrations of peptide linkages, amide II band is caused by the combination of N–H in plane bending and C–N stretching vibrations, and amide III band is caused by N–H bending vibration. Amide I band is associated with the secondary structure of protein and amide III band proved the triple-helical structure of the collagen extracted. For the pure RCSC, a strong absorption peak at 3334 cm^{-1} is caused by the stretching vibration of N–H bond of amide A. For the pure PLLA nanofibers in Figure 3(b), the strong characteristic absorption at 1759 cm^{-1} is attributed to the stretching vibration of C–O bond. VCM FTIR spectra showed the characteristic peaks of functional group COOH at 3387.38 cm^{-1}, R–CH_2–CH_3 at 2935.51 cm^{-1}, R–NH–R at 2842.19 cm^{-1}, R–CO–NH_2 at 1632.81 cm^{-1}, R–O–R at 1093.52 cm^{-1}, and R–NH_2 at 687.81 cm^{-1}. These characteristic absorption bands were also observed in the FTIR spectra of blend and coaxial RCS/PLLA (VCM) nanofiber membranes.

3.3. Thermal Behavior. DSC essays were conducted to study the effects of RCSC and VCM on the crystallization behavior of the scaffolds. DSC thermogram of pure PLLA, blend, and coaxial RCSC/PLLA nanofiber membranes is shown in Figure 4. Data of thermal properties of electrospun nanofiber membranes is shown in Table 1. The glass-transition temperature of blend and coaxial RCSC/PLLA nanofiber scaffolds ranged from 85.58°C to 97.31°C. The melting point of the pure PLLA scaffolds was 180.3°C and cold crystallization temperature is 81.72°C. In addition, after mixing the nanofiber mats with RCSC and VCM, the melting temperature is reduced and the cold crystallization temperature increased. The coaxial RCSC/PLLA scaffolds performed better crystallization property with higher degree of crystallization (17.89% and 17.24%) than the blend group (17.74% and 16.13%). The blend and coaxial RCSC/PLLA nanofiber scaffolds had lower degree of crystallinity (16.13%–17.89%) than the pure PLLA (42.63%) which may contribute to the intermolecular forces of the internal molecules in the blending and core-shell structure. For the medicine carrying RCSC/PLLA nanofiber scaffolds, the thermal properties were not distinct obviously with the nonmedicine RCSC/PLLA nanofiber scaffolds which indicated that the VCM has little effect on the thermal behavior of the RCSC/PLLA nanofiber scaffolds.

3.4. Hydrophilic Analysis. The contact angle between the electrospun scaffolds and the deionized water was measured to determine the hydrophilicity of the nanofiber scaffolds. The measured contact angle values and representative pictures in 10 seconds of the nanofiber membranes were shown in Figure 5. As seen in Figure 5(f), while the water contact angle decreased to nearly zero for the nanofiber mats containing

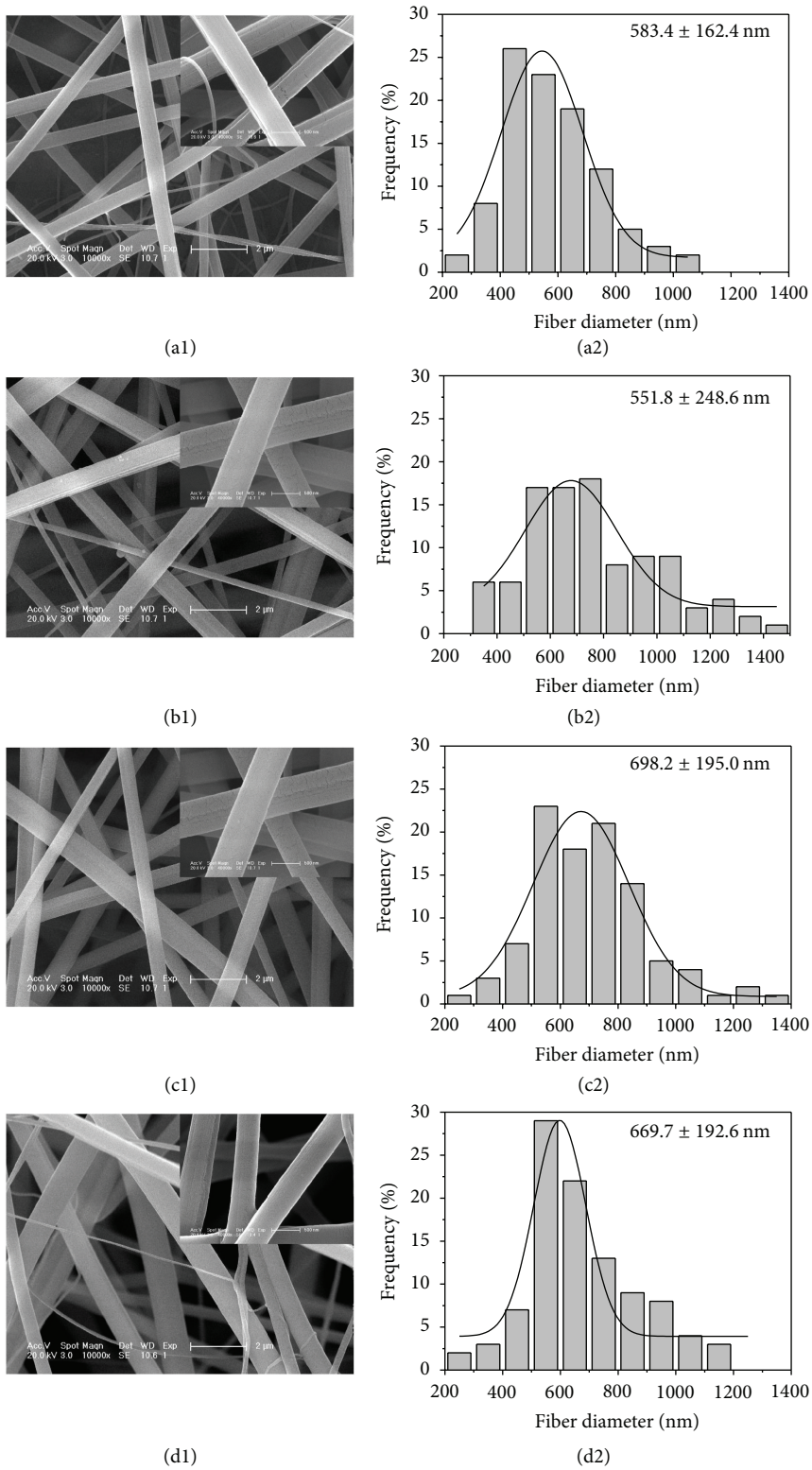

Figure 1: SEM micrographs and fiber diameter distribution of the four electrospun scaffolds: blend RCSC/PLLA (a1, a2), blend RCSC/PLLA/VCM (b1, b2), coaxial RCSC/PLLA (c1, c2), and coaxial RCSC/PLLA (VCM) (d1, d2).

Table 1: Thermal properties of electrospun nanofiber membranes.

Sample	T_g (°C)[a]	T_c (°C)[b]	ΔH_c (J/g)[c]	T_m (°C)[d]	ΔH_m (J/g)[e]	X (%)[f]
Blend RCSC/PLLA	85.58	92.44	5.27	174.21	10.22	17.74
Blend RCSC/PLLA/VCM	88.39	93.02	5.75	174.18	10.25	16.13
Coaxial RCSC/PLLA	97.31	100.71	4.84	177.35	9.83	17.89
Coaxial RCSC/PLLA (VCM)	96.10	100.73	4.69	176.70	9.50	17.24
Pure PLLA	60.53	81.72	12.66	180.3	52.31	42.63

[a]Glass-transition temperature; [b]cold crystallization temperature; [c]cold crystallization enthalpy; [d]melting temperature; [e]melting enthalpy; [f]degree of crystallinity.

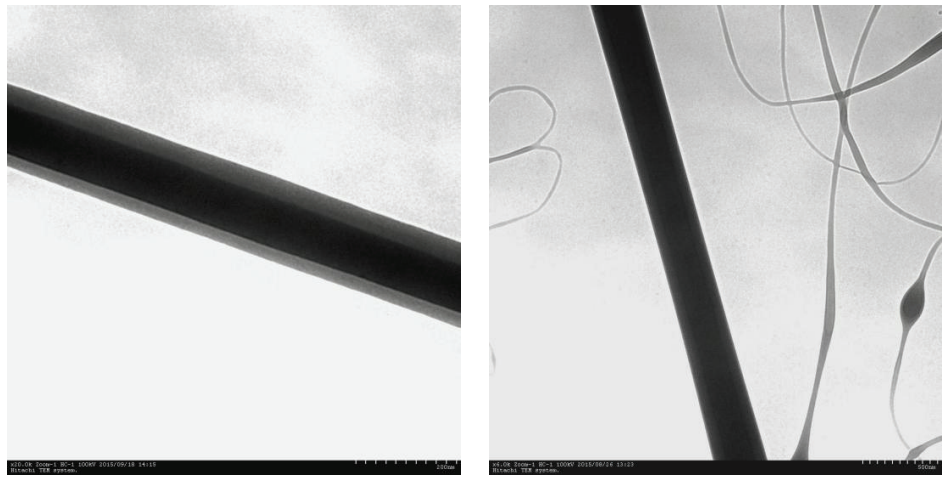

(a) (b)

Figure 2: TEM micrographs of the electrospun nanofibers: (a) coaxial RCSC/PLLA; (b) coaxial RCSC/PLLA (VCM).

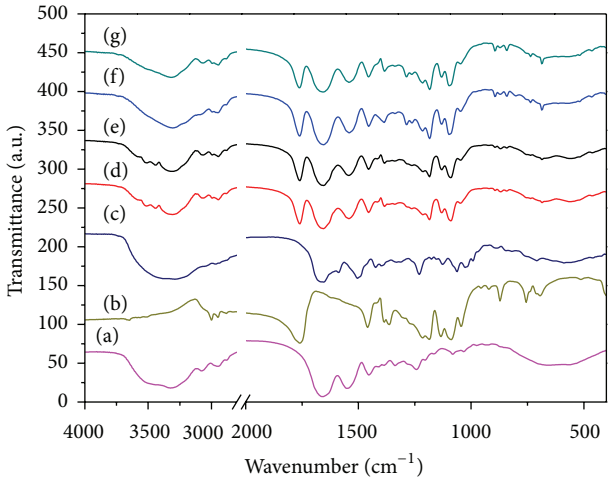

Figure 3: FTIR spectra of different nanofiber membranes: (a) RCSC; (b) PLLA; (c) VCM; (d) blend RCSC/PLLA; (e) blend RCSC/PLLA/VCM; (f) coaxial RCSC/PLLA; (g) coaxial RCSC/PLLA (VCM).

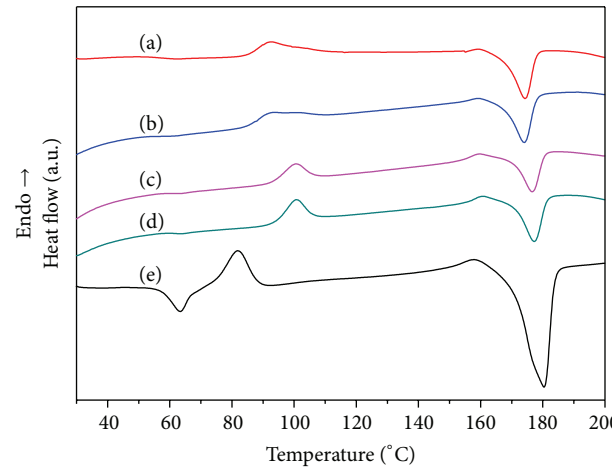

Figure 4: DSC thermograms of different nanofiber membranes: (a) blend RCSC/PLLA; (b) blend RCSC/PLLA/VCM; (c) coaxial RCSC/PLLA; (d) coaxial RCSC/PLLA (VCM); (e) pure PLLA.

only RCSC after 5 seconds, indicating that the nanofiber mats remain hydrophilic when the water droplet made a surface contact, this significant change in water contact angle is probably due to the poor morphological stability of RCSC in water as it tends to collapse into a film [24]. However, the contact angles of the pure PLLA and RCSC/PLLA nanofiber mats are between 127.12° and 116.04°, indicating

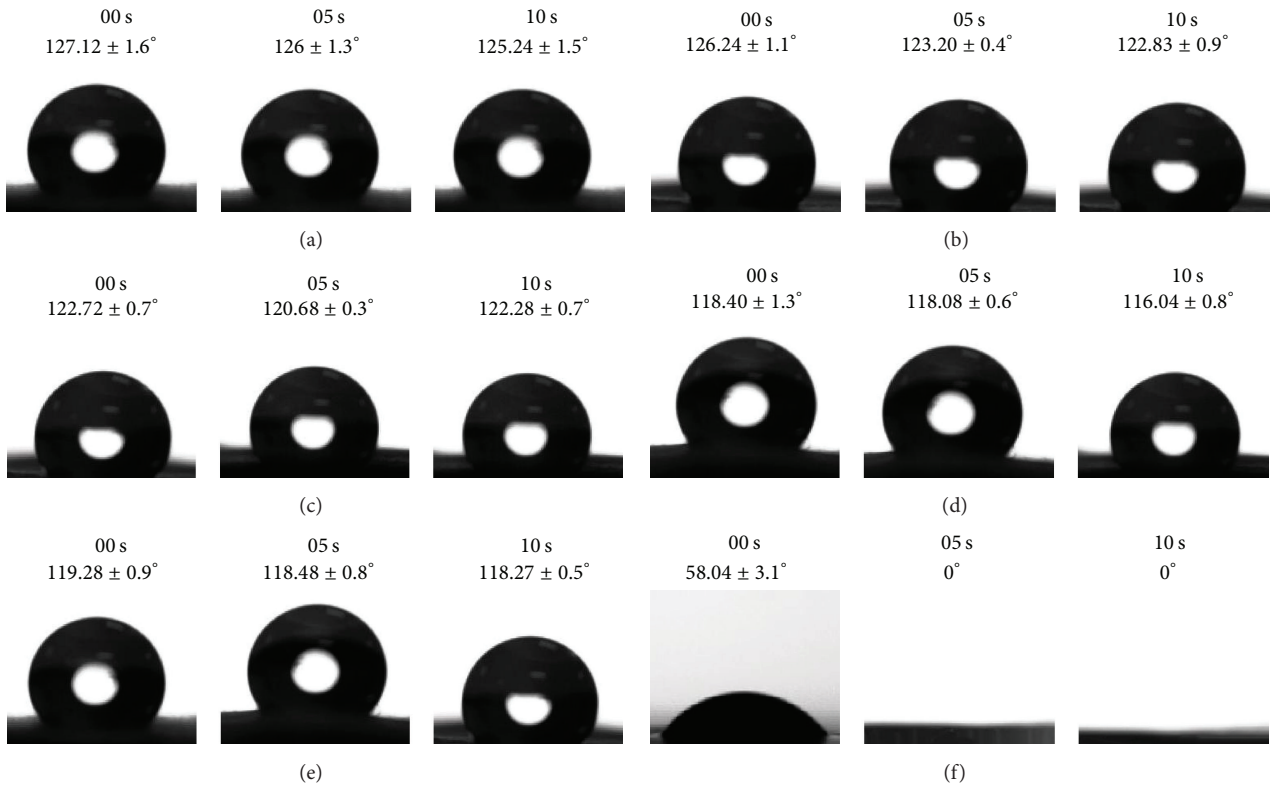

Figure 5: Contact angles of nanofiber scaffolds in pure water: (a) PLLA; (b) blend RCSC/PLLA; (c) blend RCSC/PLLA/VCM; (d) coaxial RCSC/PLLA; (e) coaxial RCSC/PLLA (VCM); (f) RCSC.

that the nanofiber membranes remain hydrophobic when the water droplet made a surface contact. This may be because the hydrophobic property of PLLA impacts more than the hydrophilic property of RCSC, making the composite RCSC/PLLA scaffolds perform hydrophobically [25]. Besides, the results demonstrated that the core-shell structure is more obvious with hydrophobicity characteristic. Pure PLLA nanofiber mats remain hydrophobic and show good morphological stability, due to the presence of methyl group in PLLA chemical structure and the lack of hydrophilic group.

3.5. Mechanical Properties. The typical stress-strain curves and mechanical properties of different nanofiber membranes were shown in Figure 6 and Table 2. Overall, the coaxial nanofiber matrix had better Young's modulus, tensile strength, and yield stress while the blend nanofiber matrix had better elongation at break. Non-VCM coaxial RCSC/PLLA scaffolds exhibited the best mechanical properties maybe due to the supporting role of PLLA in the core. With the addition of VCM, the mechanical property of coaxial nanofiber declined. The phenomenon may be explained by the existence of the VCM. It has been documented that the addition of low molecular drug had a "plasticizing" effect on fibers [26]. Therefore, the mechanical properties of the coaxial nanofibers decreased with the addition of VCM. For the blend nanofiber matrix, the mechanical properties were not distinct obviously. The result indicated that the coaxial scaffold had better mechanical properties.

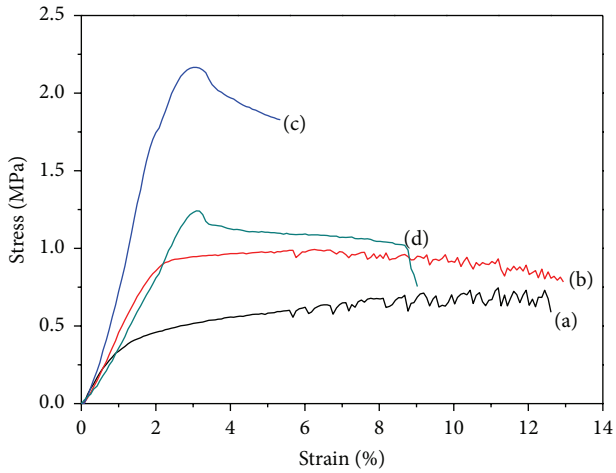

Figure 6: Typical tensile strain-stress curves of different nanofiber membranes: (a) blend RCSC/PLLA; (b) blend RCSC/PLLA/VCM; (c) coaxial RCSC/PLLA; (d) coaxial RCSC/PLLA (VCM).

3.6. Drug Release. The release behaviors of VCM from the nanofiber scaffolds were studied. As shown in Figure 7, the VCM was almost completely released within 48 hours. Both release curves exhibited high release during the first 10 hours, followed by a more gradual and sustained release of VCM. The cumulative release rate of blend RCSC/PLLA/VCM was 97% and the coaxial RCSC/PLLA (VCM) was 80%.

Table 2: Mechanical properties of different nanofiber membranes.

Sample	Young's modulus (MPa)	Tensile strength (MPa)	Elongation at break (%)
Blend RCSC/PLLA	35.86 ± 4.48	0.76 ± 0.12	12.55 ± 1.91
Blend RCSC/PLLA/VCM	25.04 ± 4.65	0.99 ± 0.09	15.67 ± 1.78
Coaxial RCSC/PLLA	109.04 ± 10.79	2.15 ± 0.39	6.32 ± 0.86
Coaxial RCSC/PLLA (VCM)	44.61 ± 11.57	1.24 ± 0.13	11.39 ± 2.04

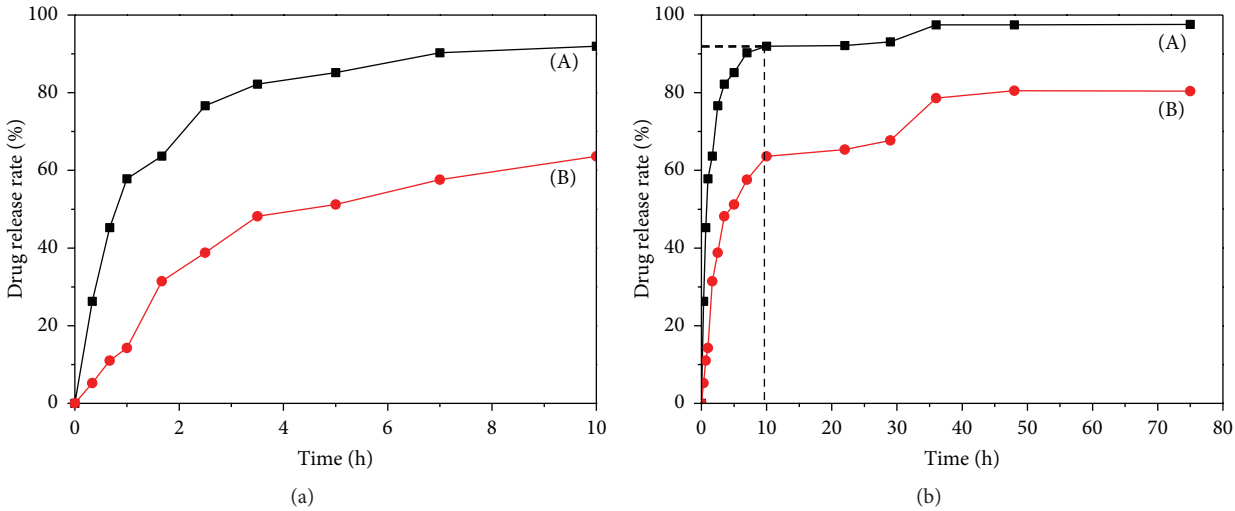

Figure 7: Drug release of VCM from nanofiber membranes: (a) blend RCSC/PLLA/VCM; (b) coaxial RCSC/PLLA (VCM).

The release rate of the coaxial RCSC/PLLA (VCM) was always lower than the blend RCSC/PLLA (VCM) at any time which indicated that VCM in nanofiber mats of core-shell structure was released more slowly. This can be explained by the fact that the surface of PLLA and RCSC blend acts as a barrier to the VCM; thus the release rate decreases. The experimental result indicated that the coaxial nanofiber might be better drug carriers for its slow-release.

4. Conclusion

In this study, we made an environment-friendly use of waste *Rana chensinensis* skin by extracting collagen from *Rana chensinensis* skin and successfully fabricated four different kinds of nanofiber mats. The SEM micrographs showed that the nanofibers had continuous and bead-free morphology and the addition of VCM decreased the nanofiber diameter. FTIR spectroscopy approved that the substance we extracted was collagen and the existence of RCSC, PLLA, or VCM in the electrospun scaffolds. DSC test showed that the carrying of VCM did not change the crystallinity of PLLA obviously. Mechanical property testing indicated that the core-shell structure nanofiber matrix is better in Young's modulus and yield stress as well as tensile strength. Both blend and coaxial nanofiber matrix showed hydrophobic property while the pure RCSC matrix showed hydrophobic property. Through the drug release experiment, the cumulative release rate of blend RCSC/PLLA/VCM scaffolds was 97% and that of the coaxial RCSC/PLLA (VCM) scaffolds was 80% which indicated that both the blend and coaxial nanofiber can be drug carriers of VCM. Overall, the coaxial RCSC/PLLA (VCM) electrospun nanofiber scaffold might be a good candidate for drug carriers for its better mechanical properties along slow-release effect.

Competing Interests

The authors declare that they have no competing interests.

References

[1] D. S. Katti, K. W. Robinson, F. K. Ko, and C. T. Laurencin, "Bioresorbable nanofiber-based systems for wound healing and drug delivery: optimization of fabrication parameters," *Journal of Biomedical Materials Research—Part B: Applied Biomaterials*, vol. 70, no. 2, pp. 286–296, 2004.

[2] M. A. Fonder, G. S. Lazarus, D. A. Cowan, B. Aronson-Cook, A. R. Kohli, and A. J. Mamelak, "Treating the chronic wound: a practical approach to the care of nonhealing wounds and wound care dressings," *Journal of the American Academy of Dermatology*, vol. 58, no. 2, pp. 185–206, 2008.

[3] F.-L. Mi, Y.-B. Wu, S.-S. Shyu et al., "Control of wound infections using a bilayer chitosan wound dressing with sustainable antibiotic delivery," *Journal of Biomedical Materials Research*, vol. 59, no. 3, pp. 438–449, 2002.

[4] R. Ghanbari, A. Ebrahimpour, A. Abdul-Hamid, A. Ismail, and N. Saari, "Actinopyga lecanora hydrolysates as natural antibacterial agents," *International Journal of Molecular Sciences*, vol. 13, no. 12, pp. 16796–16811, 2012.

[5] J. Boateng, J. Mani, and F. Kianfar, "Improving drug loading of mucosal solvent cast films using a combination of hydrophilic polymers with amoxicillin and paracetamol as model drugs," *BioMed Research International*, vol. 2013, Article ID 198137, 8 pages, 2013.

[6] S. Parveen, R. Misra, and S. K. Sahoo, "Nanoparticles: a boon to drug delivery, therapeutics, diagnostics and imaging," *Nanomedicine: Nanotechnology, Biology, and Medicine*, vol. 8, no. 2, pp. 147–166, 2012.

[7] A. Sharma, A. Gupta, G. Rath, A. Goyal, R. B. Mathur, and S. R. Dhakate, "Electrospun composite nanofiber-based transmucosal patch for anti-diabetic drug delivery," *Journal of Materials Chemistry B*, vol. 1, no. 27, pp. 3410–3418, 2013.

[8] R. Qi, X. Cao, M. Shen, R. Guo, J. Yu, and X. Shi, "Biocompatibility of electrospun halloysite nanotube-doped poly(Lactic-co-Glycolic Acid) composite nanofibers," *Journal of Biomaterials Science, Polymer Edition*, vol. 23, no. 1–4, pp. 299–313, 2012.

[9] E.-R. Kenawy, G. L. Bowlin, K. Mansfield et al., "Release of tetracycline hydrochloride from electrospun poly(ethylene-co-vinylacetate), poly(lactic acid), and a blend," *Journal of Controlled Release*, vol. 81, no. 1-2, pp. 57–64, 2002.

[10] M. van der Rest and R. Garrone, "Collagen family of proteins," *The FASEB Journal*, vol. 5, no. 13, pp. 2814–2823, 1991.

[11] K. Gelse, E. Pöschl, and T. Aigner, "Collagens—structure, function, and biosynthesis," *Advanced Drug Delivery Reviews*, vol. 55, no. 12, pp. 1531–1546, 2003.

[12] D. Liu, M. Nikoo, G. Boran, P. Zhou, and J. M. Regenstein, "Collagen and gelatin," *Annual Review of Food Science and Technology*, vol. 6, pp. 527–557, 2015.

[13] H. Wang, Z. Yu, Y. Hu et al., "Novel antimicrobial peptides isolated from the skin secretions of Hainan odorous frog, Odorrana hainanensis," *Peptides*, vol. 35, no. 2, pp. 285–290, 2012.

[14] Z. Wang, Y. Zhao, and T. Su, "Extraction and antioxidant activity of polysaccharides from Rana chensinensis skin," *Carbohydrate Polymers*, vol. 115, pp. 25–31, 2015.

[15] Z. Wang, Y. Zhao, T. Su, J. Zhang, and F. Wang, "Characterization and antioxidant activity in vitro and in vivo of polysaccharide purified from Rana chensinensis skin," *Carbohydrate Polymers*, vol. 126, pp. 17–22, 2015.

[16] X. J. Gou, X.-H. Li, T.-B. Ding et al., "Purification and characterization of an antibacterial peptide from Rana temporaria chensinensis skin," *Chemical Research in Chinese Universites*, vol. 15, no. 4, pp. 333–336, 1999.

[17] M. Zhang, J. Wang, W. Xu et al., "The mechanical property of Rana chensinensis skin collagen/poly(L-lactide) fibrous membrane," *Materials Letters*, vol. 139, pp. 467–470, 2015.

[18] D. Shan, Y. Shi, S. Duan, Y. Wei, Q. Cai, and X. Yang, "Electrospun magnetic poly(l-lactide) (PLLA) nanofibers by incorporating PLLA-stabilized Fe_3O_4 nanoparticles," *Materials Science and Engineering C*, vol. 33, no. 6, pp. 3498–3505, 2013.

[19] T. L. Smith, M. L. Pearson, K. R. Wilcox et al., "Emergence of vancomycin resistance in *Staphylococcus aureus*," *The New England Journal of Medicine*, vol. 340, no. 7, pp. 493–501, 1999.

[20] D. W. Chen, Y.-H. Hsu, J.-Y. Liao, S.-J. Liu, J.-K. Chen, and S. W.-N. Ueng, "Sustainable release of vancomycin, gentamicin and lidocaine from novel electrospun sandwich-structured PLGA/collagen nanofibrous membranes," *International Journal of Pharmaceutics*, vol. 430, no. 1-2, pp. 335–341, 2012.

[21] H. L. Jiang, Y. Hu, Y. Li, P. Zhao, K. Zhu, and W. Chen, "A facile technique to prepare biodegradable coaxial electrospun nanofibers for controlled release of bioactive agents," *Journal of Controlled Release*, vol. 108, no. 2-3, pp. 237–243, 2005.

[22] L. Zhang, J. Yan, Z. Yin et al., "Electrospun vancomycin-loaded coating on titanium implants for the prevention of implant-associated infections," *International Journal of Nanomedicine*, vol. 9, no. 1, pp. 3027–3036, 2014.

[23] K. Belbachir, R. Noreen, G. Gouspillou, and C. Petibois, "Collagen types analysis and differentiation by FTIR spectroscopy," *Analytical and Bioanalytical Chemistry*, vol. 395, no. 3, pp. 829–837, 2009.

[24] S. Ali, Z. Khatri, K. W. Oh, I.-S. Kim, and S. H. Kim, "Zein/cellulose acetate hybrid nanofibers: electrospinning and characterization," *Macromolecular Research*, vol. 22, no. 9, pp. 971–977, 2014.

[25] S. Maretschek, A. Greiner, and T. Kissel, "Electrospun biodegradable nanofiber nonwovens for controlled release of proteins," *Journal of Controlled Release*, vol. 127, no. 2, pp. 180–187, 2008.

[26] S. Shao, L. Li, G. Yang et al., "Controlled green tea polyphenols release from electrospun PCL/MWCNTs composite nanofibers," *International Journal of Pharmaceutics*, vol. 421, no. 2, pp. 310–320, 2011.